LABORATORY MEASUREMENT OF SEDIMENT TRANSPORT UNDER A BREAKING WAVE TURBULENT FLOW FIELD

Junichi Otsuka[1], Yasunori Watanabe[2]

Instantaneous velocity fields and suspended sediment concentration in surf zones were measured in a wave flume with a sloped sand bed by use of a particle image velocimetry (PIV) and an optical concentration sensor. This was done in order to elucidate sediment transport processes and clarify the relationship between kinetic turbulent energy and sediment suspension under a breaking wave turbulent flow field. In surf zones, sediments become highly suspended when strong turbulent energy reaches the bottom. High concentration was seen in the transition region where turbulent energy is at its maximum. Suspended sediment concentration in a plunging breaker is much higher than that in a spilling breaker because large-scale vortices are typically developed and stir-up much sediment. Suspended sediment is transported to a deeper region due to the undertow becoming highly developed after a wave crest has passed. In shallower regions, suspended sediment concentration increases linearly with an increasing of the turbulent energy. The slope of the approximation line for plunging breakers is steeper than that for spilling breakers.

Keywords: breaking wave, suspended sediment, turbulent energy, particle image velocimetry (PIV)

INTRODUCTION

Sediment transport processes in surf zones have been extensively studied in laboratory experiments and field observations in recent decades. However, it is not possible to accurately predict sediment transport rates because the sediment transport processes seen under breaking wave turbulent flows, which essentially cause sediment suspension and diffusion, have not been clarified quantitatively. In surf zones, plunging jets of breaking waves sequentially splash onto the water surface ahead, producing horizontal roller vortices and obliquely descending eddies (Nadaoka et al., 1989). These vortices generate three-dimensional, strong turbulent flows, thereby enhancing sediment suspension and diffusion, and evolve into turbulent bores with wave propagation. The process of development for these vortices varies by breaker type; typically either with spilling or plunging breakers. Turbulent flow fields in surf zones have been experimentally investigated using a laser-Doppler velocimeter (LDV) (e.g. Ting and Kirby, 1994; Cox and Kobayashi, 2000) and a particle image velocimetry (PIV) (e.g. Cox and Anderson, 2001; Kimmoun and Branger, 2007; Huang et al., 2009). These studies presented turbulence properties under breaking waves in detail. However, the relationship between turbulence intensity and sediment suspension rates has not been clarified because these laboratory experiments were conducted in a wave flume with a sloped fixed bed.

In this study, velocity fields and suspended sediment concentrations in surf zones were measured in a wave flume with a sloped sand bed using a PIV system and an optical concentration sensor in order to elucidate sediment transport processes in surf zones and to clarify the relationship between kinetic turbulent energy and sediment suspension under breaking waves.

EXPERIMENTAL SETUP FOR PIV MEASUREMENTS

The experiments were performed in a glass side walled wave flume: 24.0 m in length, 0.4 m in width and 1.0 m in depth (Figure 1). Waves were generated by a piston-type wave generator set up at one end of the wave flume. The still water depth in the constant-depth section of the wave flume was 0.6 m. A well-sorted sand bed was installed in the flume to create a uniform 1:20 beach slope. The median grain diameter (d_{50}) of the sand bed was 0.20 mm. The velocity fields on the vertical plane crossing the beach in the surf zones were measured using a PIV system. A high-speed video camera (FASTCAM-SA3, Photron) and a green laser sheet (DPGL-8W, JAPAN LASER) were used in the PIV measurements. The field of view (FOV) for the camera covered a region of 12 cm (length)$\times$6 cm (height), including the bottom level (Figure 2). The FOV was set at 7 cm parallel to the sidewall of the flume, and was irradiated with the laser sheet 30 cm offshore from the center of the FOV. The FOV was traversed from the wave breaking point toward the shoreline at 10 cm intervals. The image acquisition frequency was 250 Hz, and the image resolution was 1024 pixels (length) $\times$ 512 pixels (height). For the PIV measurements, the window size was 31 $\times$ 31 pixels and the size of the interrogation region was 73$\times$73 pixels. The window was overlapped at 15 pixel intervals. The water surface elevation at each FOV was measured with a capacitance-type wave gage set at 23 cm from the center of the FOV in the transverse direction of the wave flume (Figure 2). The wave data acquisition frequency was 100 Hz. The high-speed video camera and the wave gage were simultaneously triggered by a TTL signal generated when a wave gage installed in front of the wave generator detected the first

[1] Civil Engineering Research Institute for Cold Region, Hiragishi 1-3-1, Sapporo, 060 8628 Japan
[2] School of Engineering, Hokkaido University, North 13 West 8, Sapporo, 060 8628 Japan

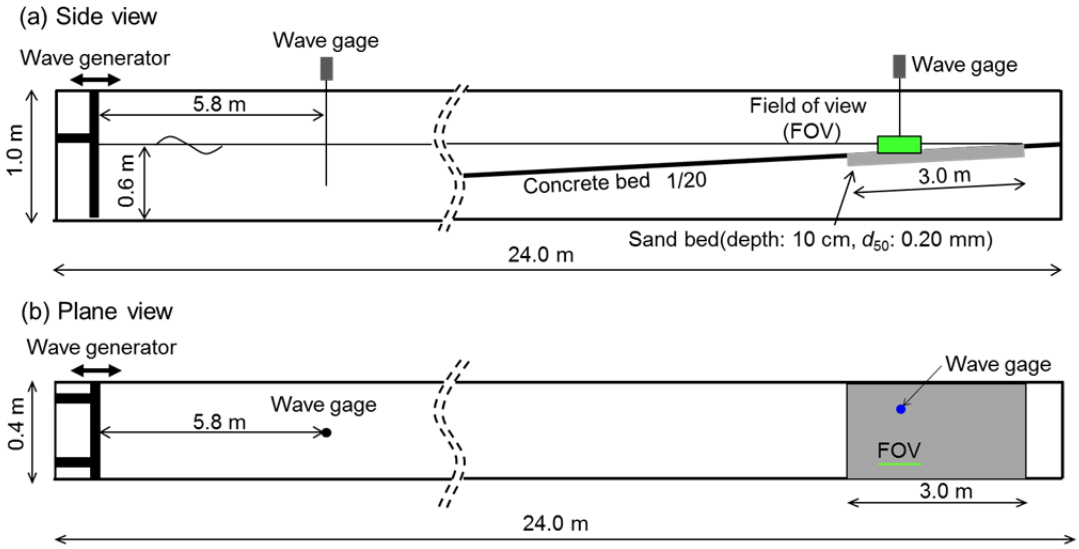

Figure 1. Experimental setup for PIV measurements.

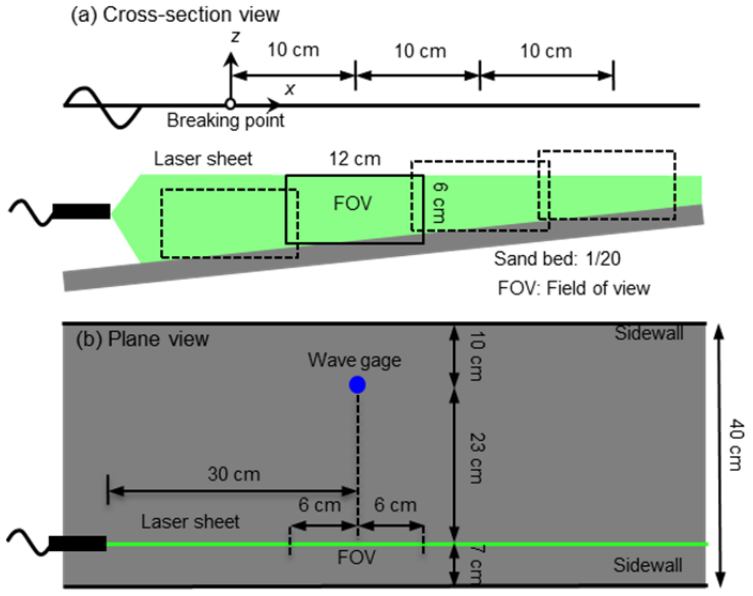

Figure 2. Enlarged view around the PIV measurement region.

wave.

For the PIV measurements, fluorescent buoyant tracers of 60−200 μm in diameter were seeded in the wave flume, which were excited by green laser light at a wavelength of 532 nm (Figure 3). The peak wavelength of the excitation lights from the tracers was 650 nm. Suspended sediment in the FOV reflects the green laser light from their surfaces. To capture only laser-induced fluorescent (red) light from the tracers, a high-pass optical filter, with a cut-off wavelength of lower than 580 nm, was attached to the camera lens.

EXPERIMENTAL SETUP FOR MEASUREMENTS OF SUSPENDED SEDIMENT

These experiments were conducted in the same wave flume used in the PIV measurements. Suspended sediment concentration was measured using an optical concentration sensor (PMT5-50, KENEK) at the same locations as the PIV measurements (Figure 4). The measurement points were located at 10 cm intervals from the wave breaking point toward the shoreline, along the centerline of the wave flume. At each location, the concentration was measured at one to five elevations from 1 cm

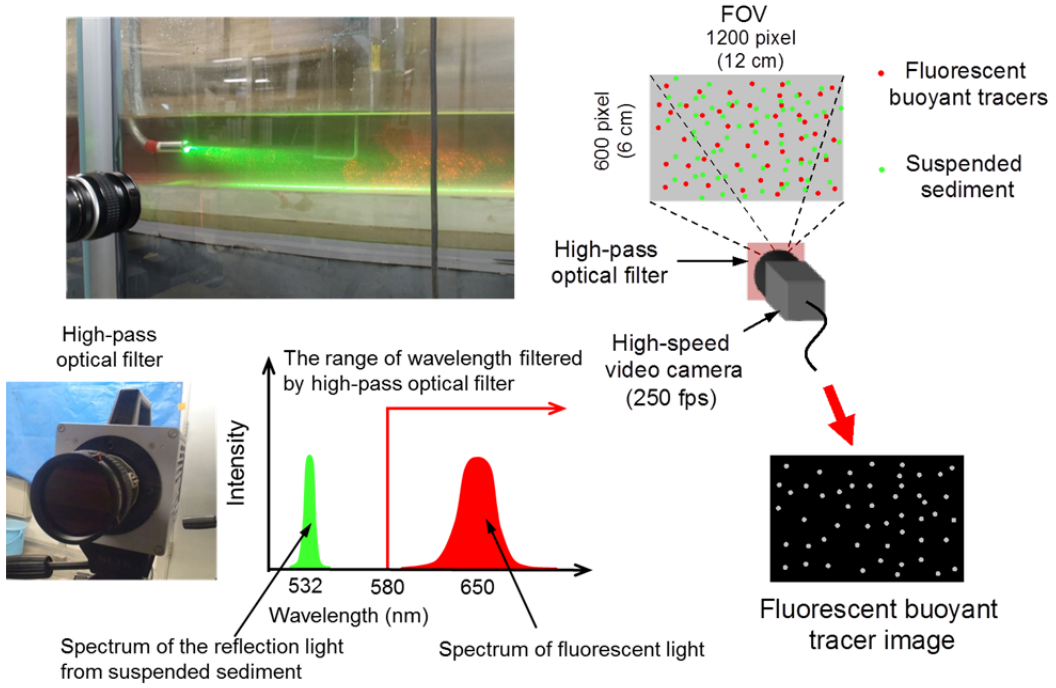

Figure 3. Optical filtering technique for recording the only fluid motion.

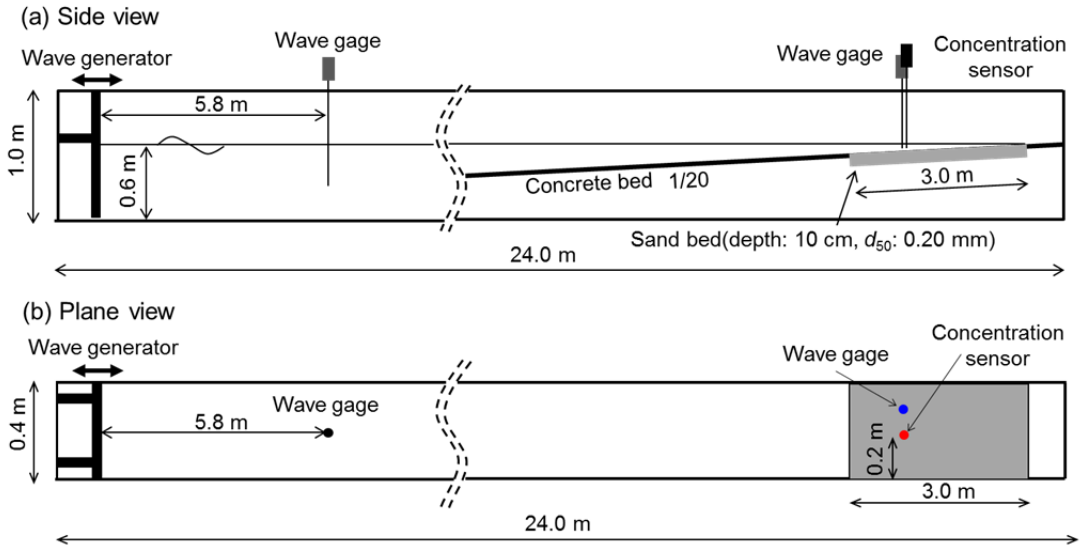

Figure 4. Experimental setup for measurements of suspended sediment concentration.

above the bottom below the wave trough level (Figure 5). A wave gage was set at the same locations as the PIV measurements. The data acquisition frequency of these instruments was 100 Hz. Both instruments were triggered by the TTL signal, as in the PIV measurements.

EXPERIMENTAL CONDITIONS

Both experiments were conducted with three regular wave conditions as shown in Table 1.The major factors considered were the wave period T (or the deep-water wavelength L_0 via the dispersion relationship), the breaking wave height H_b, the breaking water depth h_b and the bottom slope θ. The surf similarity parameter ξ was given as $\xi = \tan\theta/\sqrt{H_b/L_0}$. The wave breaker types were a spilling breaker in Case 1and a plunging breaker in Case 2. Waves were generated for 30 seconds and the sand bed was flattened after wave generation. As the bed form changed little throughout the period, bed

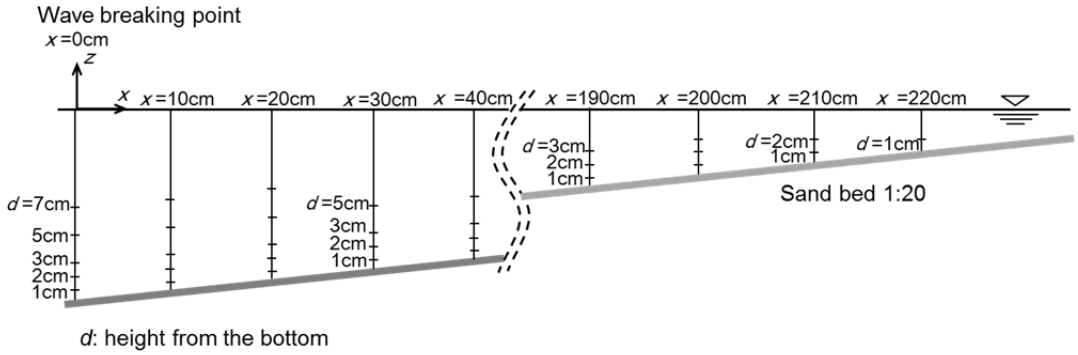

Figure 5. Measurement locations for suspended sediment concentration.

Table 1. Experimental wave conditions (*T*: wave period; H_b: breaking wave height; h_b: breaking water depth).

	T (s)	H_b (cm)	h_b (cm)	Bottom slope	Surf similarity parameter	Breaker type
CASE 1	1.4	12.5	13.8	1/20	0.247	Spilling
CASE 2	2.0	13.7	14.1	1/20	0.337	Plunging

features such as ripples were not considered in this study. More than 30 measurements for the PIV, suspended sediment concentration and water surface elevation were made at each location to obtain the ensemble-averaged velocity, concentration and wave fields in the surf zones.

The horizontal coordinate x was defined as positive onshore, with $x = 0$ at the wave breaking point for each wave condition. The vertical coordinate z was defined as positive upward with $z = 0$ at the still water level.

RESULTS

Figure 6 and Figure 7 show temporal variations in the cross-shore distributions of ensemble-averaged: (a) surface elevation, (b) velocity and turbulent energy, and (c) suspended sediment concentration in Case1 (spilling breaker), and Case2 (plunging breaker). In these figures, waves propagate: (1) near the wave breaking point, (2) in transition region and (3) in bore region. Turbulent energy is defined as $k = (\overline{u'^2}+\overline{v'^2})/2$, where $u' = u - \bar{u}$, $v' = v - \bar{v}$. The symbol $\bar{}$, u and v denote ensemble-averaging operation for instantaneous values, horizontal velocity and vertical velocity, respectively.

In the spilling breaker (Figure 6), a wave crest spills down the water surface ahead to produce smaller roller vortices. Initially, only weak turbulence is generated in the vicinity of the water surface, and this gradually develops into turbulent bores with wave propagation. The weak turbulence generated in the deeper region cannot easily reach the bottom. In the transition region and bore region, turbulent energy is provided from the water surface toward the bottom after a wave crest has passed. A number of sediments are suspended from the bottom when intense turbulent energy reaches the bottom. These suspended sediments are transported to a deeper region, in the offshore direction,while the undertow is highly developed. The turbulent energy is almost dissipated before the arrival of the next wave.

In a plunging breaker (Figure 7), higher concentrations are seen near the bottom in the transition region where turbulent energy is at its maximum because large-scale vortices with horizontal roller vortices and obliquely descending eddies typically develop and stir up large amounts of sediment. As dynamic splash-up continues from the transition region toward the bore region, successive plunging jets affect to stir up sediment. Less turbulent energy is provided from the water surface in the bore region than in the transition region because turbulence generated in the latter fully evolves into turbulent bores with wave propagation. The concentration in the shallower region is relatively higher than that in a spilling breaker. The suspended sediments are transported toward the deeper region by undertow, and tend to concentrate around the wave plunging point. The intense turbulent energy declines in strength while the undertow is developed.

Figure 8 shows the cross-shore distributions of time-averaged turbulent energy and suspended sediment concentration at 1 cm above the bottom in Case1 and Case 2. The horizontal axis is expressed

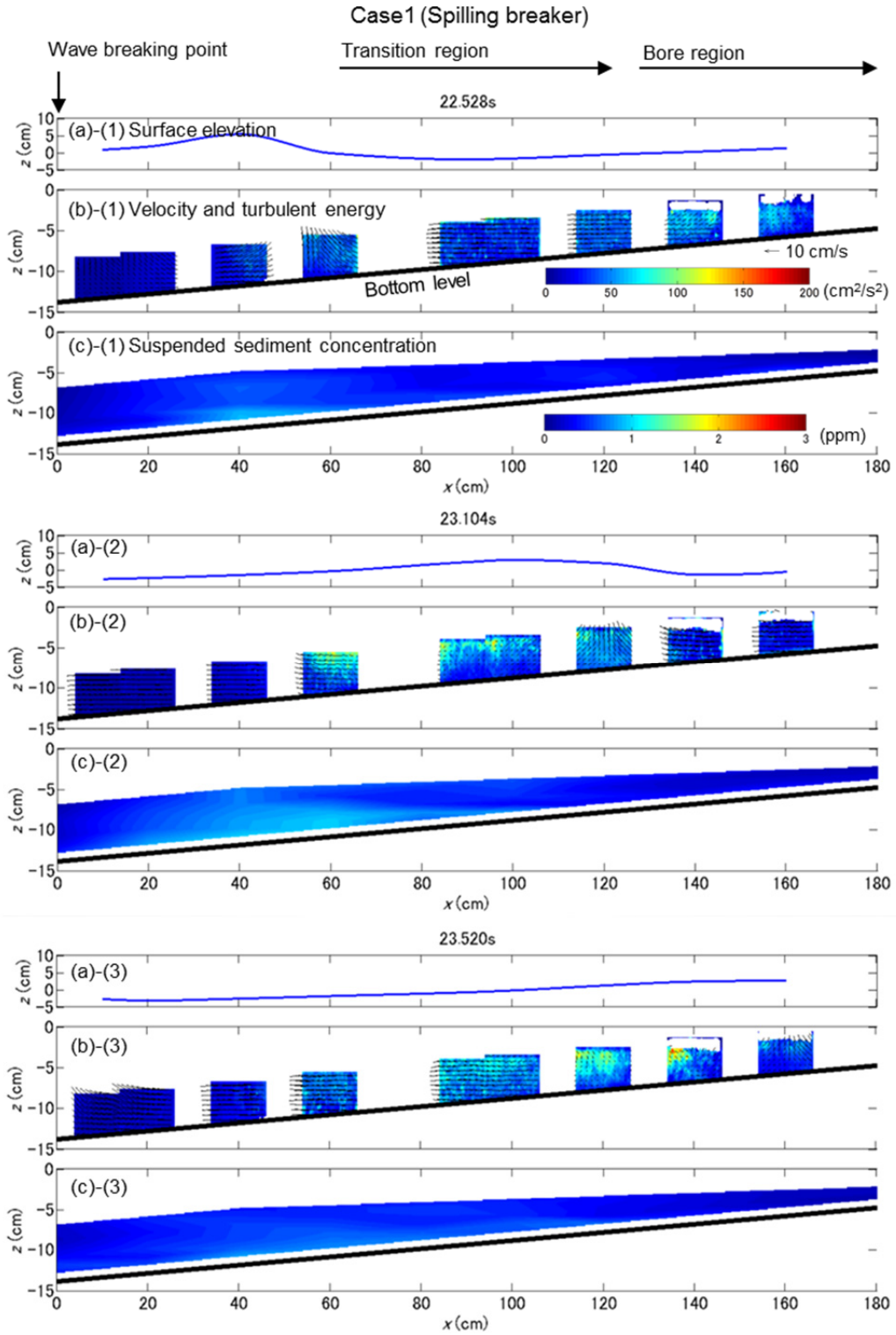

Figure 6. Temporal variations in the cross-shore distributions of ensemble-averaged (a) surface elevation, (b) velocity and turbulent energy and (c) suspended sediment concentration in Case1 (The wave propagates (1) near the wave breaking point, (2) in transition region and (3) in bore region).

as non-dimensional parameter x / h_b, where x is distance from the wave breaking point and h_b is breaking water depth. As mentioned in Figure 6 and Figure 7, suspended sediment is transported to deeper a region by the undertow. Therefore, even though little turbulent energy is provided, the concentration increases with time in a deeper region. Our discussion will focus on the relationship

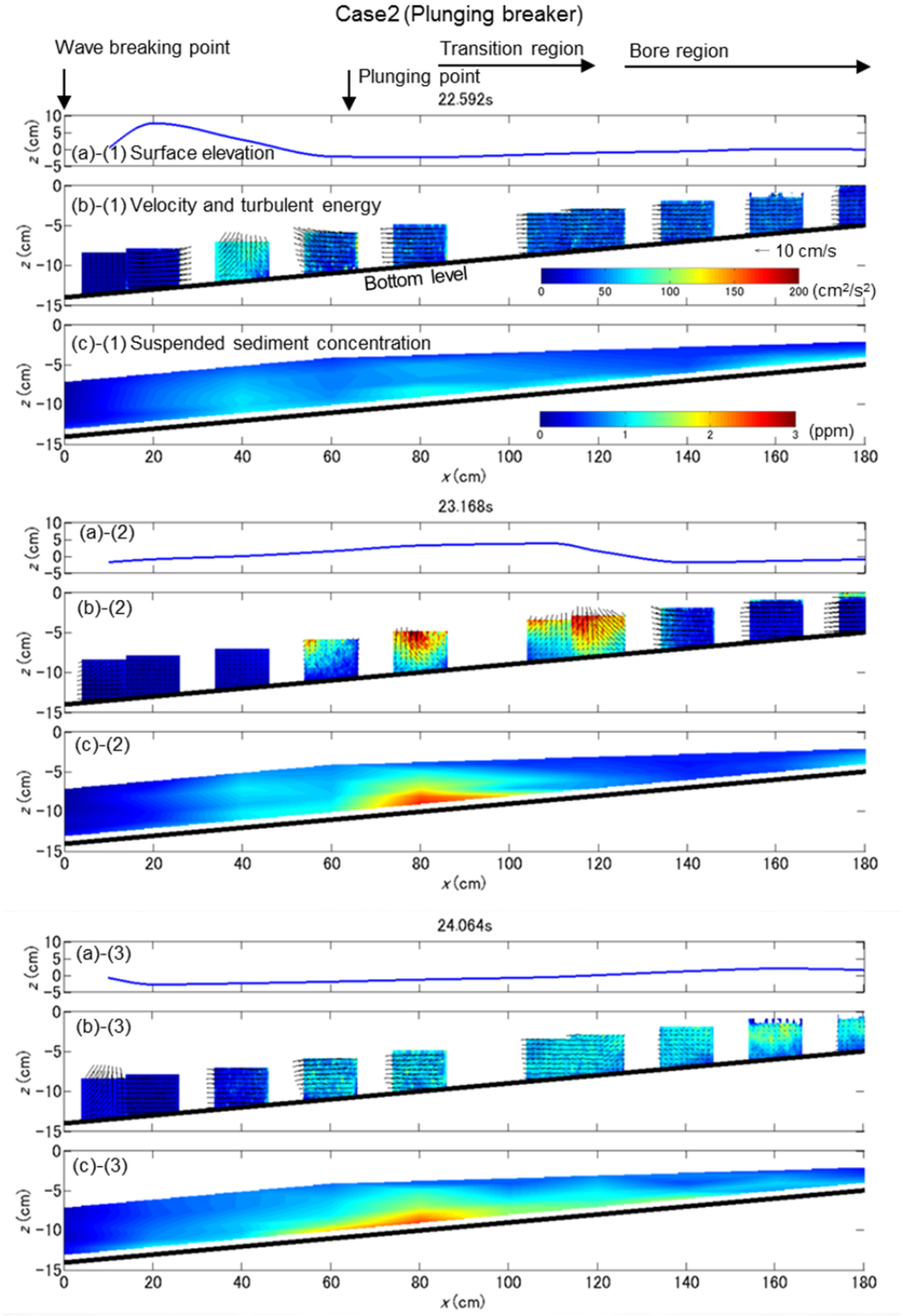

Figure 7. Temporal variations in the cross-shore distributions of ensemble-averaged (a) surface elevation, (b) velocity and turbulent energy and (c) suspended sediment concentration in Case2 (The wave propagates (1) near the wave breaking point, (2) in transition region and (3) in bore region).

between turbulent energy and suspended sediment concentration only in shallower regions, where x / h_b is greater than 5. In the shallower region, as the turbulent energy decreases, the concentration also decreases. The concentration in a plunging breaker is much higher than that in a spilling breaker.

Figure 9 shows the relationship between the time-averaged turbulent energy and suspended

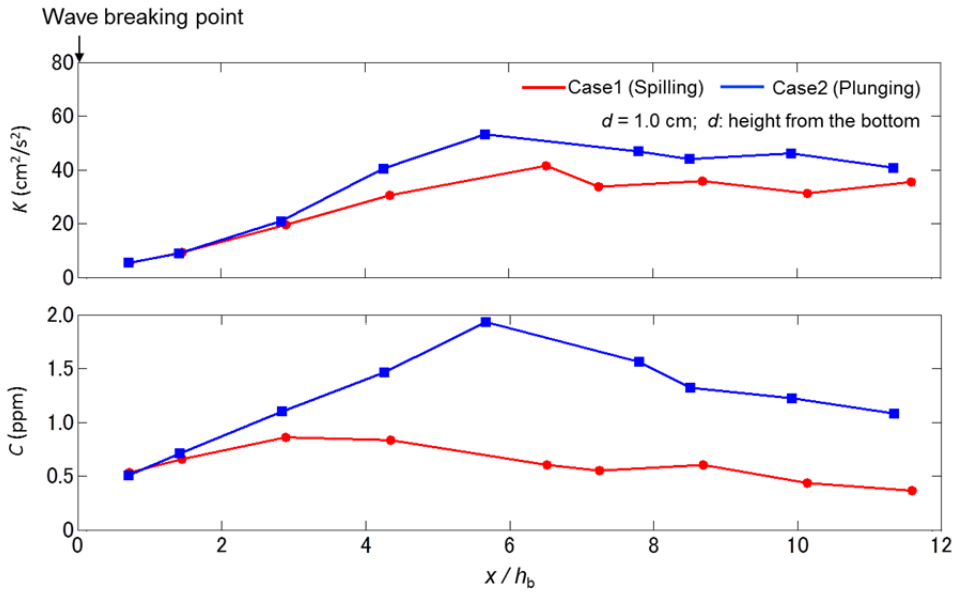

Figure 8. Cross-shore distributions of time-averaged turbulent energy and suspended sediment concentration at 1cm above the bottom (*x*: distance from the wave breaking point, h_b: breaking water depth).

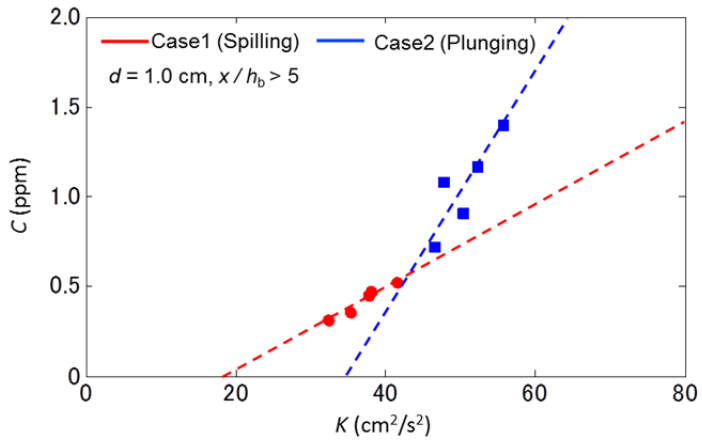

Figure 9. Relationship between time-averaged turbulent energy and suspended sediment concentration at 1 cm above the bottom in shallower region, where x / h_b is greater than 5.

sediment concentration at 1 cm above the bottom in the shallower region, where x / h_b is greater than 5, as mentioned in Figure 8. In the both cases, the concentration increases with increasing of the turbulent energy. The slope of the approximation line for a plunging breaker is much steeper than that for a spilling breaker. It can be said that breaker type is an important factor for sediment suspension under breaking wave turbulent flows, particularly in shallower regions.

CONCLUSIONS

Instantaneous velocity fields and suspended sediment concentration were investigated in laboratory surf zones using a PIV system with an optical filtering technique and an optical concentration sensor. In surf zones, turbulent energy is provided from the waver surface toward the bottom after a wave crest passed. The turbulence intensity reached at its maximum in the transition region and gradually decreased with wave propagation. The turbulent energy is almost dissipated before the arrival of the next wave. Sediments are highly suspended when strong turbulent energy reaches the bottom. High concentration was seen in the transition region where turbulent energy is at its

maximum. Suspended sediment concentration in a plunging breaker is much higher than that in a spilling breaker because large-scale vortices are typically developed and stir-up much sediment in the plunging breaker. The concentration in deeper regions increases with time, even though less turbulent energy is provided, because suspended sediment is transported to the deeper region by undertow. In shallower regions where x / h_b is greater than 5, suspended sediment concentration linearly increases with increasing of the turbulent energy. The slope of the approximation line for a plunging breaker is steeper than that for a spilling breaker.

ACKNOWLEDGMENTS

Financial support for this study was provided by a JSPS Grant-in-Aid for Scientific Research (22760378).

REFERENCES

Cox, D.T. and Kobayashi, N., 2000, Identification of intense, intermittent coherent motions under shoaling and breaking waves, *Journal of Geophysical Research,* 105, C6, 223-236.

Cox, D.T. and Anderson, S.L., 2001, Statistics of intermittent surf zone turbulence and observations of large eddies using PIV, *Coastal Engineering Journal,* 43, 121-131.

Huang, Z.C., Hwung, H.H., Hsiao, S.C. and Chang, K.A., 2009, Turbulence and energy dissipations of surf-zone spilling breakers, *Coastal Engineering*, 56, 733-746.

Kimmoun, O. and Branger, H., 2007, A particle images velocimetry investigation on laboratory surf-zone breaking waves over a sloping beach, *Journal of Fluid Mechanics*, 588, 353-397.

Nadaoka, K., Hino, M. and Koyano, Y., 1989, Structure of the turbulent flow field under breaking waves in the surf zone, *Journal of Fluid Mechanics,* 204, 359-387.

Ting, F.C.K. and Kirby, J.T., 1994, Observation of undertow and turbulence in a laboratory surf zone, *Coastal Engineering*, 24, 51-80.